frontiers | Frontiers in Marine Science

TYPE Original Research
PUBLISHED 12 September 2024
DOI 10.3389/fmars.2024.1445071

OPEN ACCESS

EDITED BY
Xingru Feng,
Chinese Academy of Sciences (CAS), China

REVIEWED BY
Aifeng Tao,
Hohai University, China
Jian Shi,
National University of Defense Technology, China

*CORRESPONDENCE
Hailun He
hehailun@sio.org.cn

RECEIVED 06 June 2024
ACCEPTED 21 August 2024
PUBLISHED 12 September 2024

CITATION
He H, Ling Z, Wu S, Lyu X, Zeng Z, Tian R, Wang Y and Sun J (2024) *In situ* observation of ocean response to tropical cyclone in the western North Pacific during 2022. *Front. Mar. Sci.* 11:1445071. doi: 10.3389/fmars.2024.1445071

In situ observation of ocean response to tropical cyclone in the western North Pacific during 2022

Hailun He[1,2*], Zheng Ling[3], Shouchang Wu[4], Xinyan Lyu[5], Zheng Zeng[6], Ruizhen Tian[1], Yuan Wang[7] and Jia Sun[8]

[1]State Key Laboratory of Satellite Ocean Environment Dynamics, Second Institute of Oceanography, Ministry of Natural Resources, Hangzhou, China, [2]Southern Marine Science and Engineering Guangdong Laboratory (Zhuhai), Zhuhai, China, [3]Key Laboratory of Climate, Resources and Environment in Continental Shelf Sea and Deep Sea of Department of Education of Guangdong Province, College of Ocean and Meteorology, Guangdong Ocean University, Zhanjiang, China, [4]Marine Academy of Zhejiang Province, Hangzhou, China, [5]National Meteorological Center, China Meteorological Administration, Beijing, China, [6]School of Oceanography, Shanghai Jiao Tong University, Shanghai, China, [7]Key Laboratory of Submarine Geosciences, Second Institute of Oceanography, Ministry of Natural Resources, Hangzhou, China, [8]First Institute of Oceanography, and Key Laboratory of Marine Science and Numerical Modeling, Ministry of Natural Resources, Qingdao, China

We deployed 8 surface drifters in the western North Pacific in 2022. By integrating the Global Drifter Program's data, we analyzed the drifter-based sea surface currents and temperatures during tropical cyclones. The maximum *in-situ* surface current observed was 0.70 m/s during typhoon Hinnamnor. Our surface drifters provided similar observations as compared to an adjacent Global Drifter Program's drifter. Furthermore, we investigated float profiling observations during tropical cyclones. Based on Argo float 2903647, the SST decreased by 1.4oC after the passage of typhoon Hinnamnor. This study demonstrates the reliability of our newly deployed surface drifters and exhibits the state-of-the-art capability for *in-situ* observations of tropical cyclone-ocean interaction.

KEYWORDS

surface drifter, Argo float, *in situ* observation, tropical cyclone, western North Pacific

1 Introduction

Tropical cyclones (TCs) typically originate in warm sea surface conditions (Gray, 1998). The ocean's response to TCs is intense, particularly on surface currents and temperatures (Price, 1981; Lenain and Melville, 2014). Significant cooling of sea surface temperature is mainly observed around TC paths (Oey, 2023). Observing the ocean's

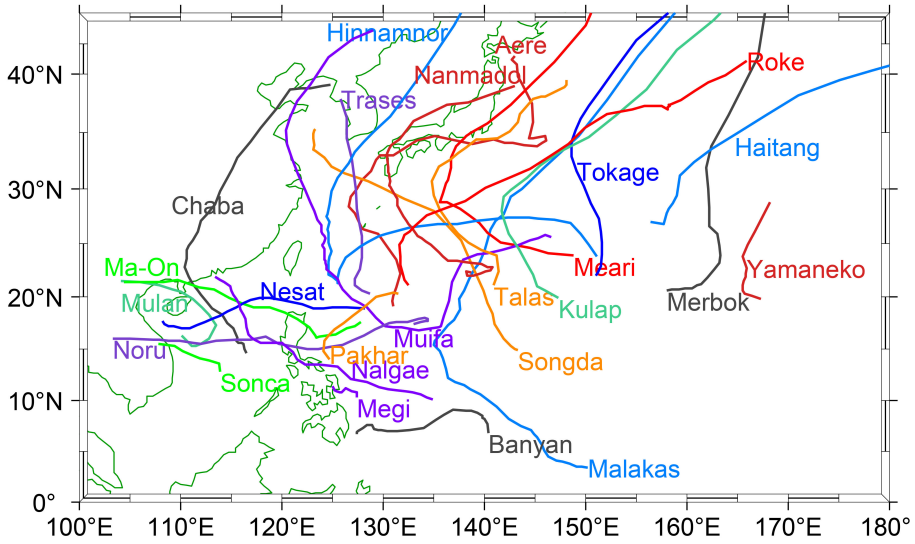

FIGURE 1
Best tracks of TCs in the western North Pacific during 2022. The best tracks were provided by Japan Meteorological Agency (JMA).

response and its feedback to TCs is crucial for understanding extreme air-sea interactions (Prasad and Hogan, 2007; Cao et al., 2022; Li et al., 2023), as well as for operational TC forecasting (Bender et al., 2007).

Strong ocean currents pose a significant risk to ocean engineering structures (Tavakoli et al., 2023), yet they also offer opportunities for renewable energy generation. Satellite altimeters provide a solution for measuring geostrophic currents (Deng, 2016). Additionally, the Geostationary Ocean Color Imager serves as a high resolution foundation for retrieving surface currents (Choi and Kim, 2018). High-frequency radar is widely employed for surface current measurements at scales of 100 km (Röhrs et al., 2015). However, *in-situ* sensor measurements of ocean currents are relatively costly (Sanford et al., 2011; He et al., 2022). Lagrangian tracking offers an alternative method for computing surface currents, leveraging satellite-based positioning systems, which are relatively reliable in terms of limited position error and real-time data transmission (Hansen and Poulain, 1996; Lumpkin and Johnson, 2013). Therefore, surface drifters, which measure Lagrangian currents, are widely used for *in-situ* surface current estimation (Laurindo et al., 2017).

TC-induced surface currents can reach speeds as high as 1 m/s (Fan et al., 2022; Yu et al., 2020). Surface drifters have been used to describe the spatial pattern of surface currents during TC events (Chang et al., 2013). However, the sparse distribution of surface drifters limits their ability to fully resolve TC cases (Chen et al., 2021; He et al., 2024). Therefore, additional surface drifters are required for more detailed TC case studies.

Recently, we deployed 8 surface drifters in the western North Pacific, each equipped with following advantageous features:

- The data were transmitted to land in real-time.
- The temporal resolution is as high as hourly.

Some of our drifters are influenced by TCs, however, their reliability for TC observation remains uncertain. This paper is

TABLE 1 Best tracks of TCs in 2022.

ID	Name	Genesis time	Life cycle	P^{min}
		YYYY-MM-DD HH	days	hPa
1	Malakas	2022-04-06 06	11.75	945
2	Megi	2022-04-08 18	3.25	996
3	Chaba	2022-06-28 18	9.00	965
4	Aere	2022-06-30 12	10.00	994
5	Songda	2022-07-26 12	5.75	996
6	Trases	2022-07-29 12	3.25	998
7	Mulan	2022-08-08 00	3.25	994
8	Meari	2022-08-08 18	8.00	988
9	Ma-On	2022-08-21 00	5.00	985
10	Tokage	2022-08-21 06	5.75	970
11	Hinnamnor	2022-08-27 18	12.25	920
12	Muifa	2022-09-03 18	13.25	950
13	Merbok	2022-09-10 12	6.25	940
14	Nanmadol	2022-09-12 12	7.50	910
15	Talas	2022-09-20 18	6.75	1000
16	Noru	2022-09-21 06	8.00	940
17	Kulap	2022-09-25 00	6.50	940
18	Roke	2022-09-28 00	7.25	975
19	Sonca	2022-10-13 06	1.75	998
20	Nesat	2022-10-14 12	5.75	965
21	Haitang	2022-10-17 00	3.50	1004
22	Nalgae	2022-10-26 00	8.00	975

(Continued)

TABLE 1 Continued

ID	Name	Genesis time	Life cycle	P^{min}
		YYYY-MM-DD HH	days	hPa
23	Banyan	2022-10-28 06	5.75	1002
24	Yamaneko	2022-11-11 12	3.25	1004
25	Pakhar	2022-12-10 00	2.50	998

P^{min} is the minimum pressure of TC center during the TC life. The data were provided by JMA.

largely motivated by this uncertainty. We aim to compare the measurement of our drifters with that of other drifters. On the other hand, in 2022, typhoon Hinnamnor proved to be particularly challenging due to its unpredictable nature. The unusual meridional turning in the western North Pacific presented a significant obstacle for track forecasting (Wang et al., 2023b, 2023a). Air-sea interaction likely contributed to its intensity change. Notably, our drifters were deployed during this typhoon event. Cases like Hinnamnor, characterized by sudden

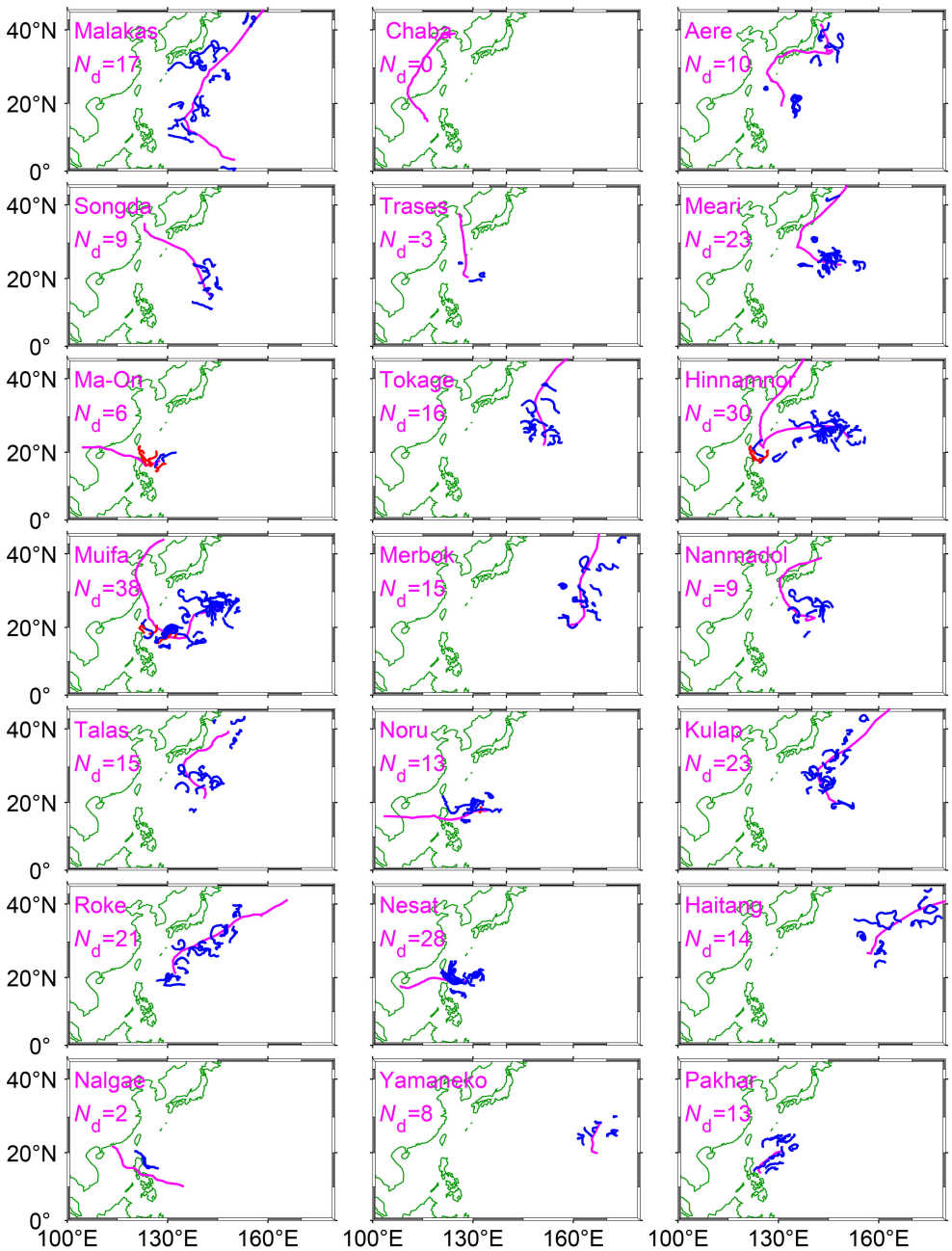

FIGURE 2
An overview of surface drifters during TCs in 2022. The magenta solid line depicts the best track of the TC, while the blue and red lines represent the trajectories of surface drifters in Global Drifter Program and our deployment, respectively. N_d is the number of captured surface drifters. The search radius is 500 km.

10.3389/fmars.2024.1445071

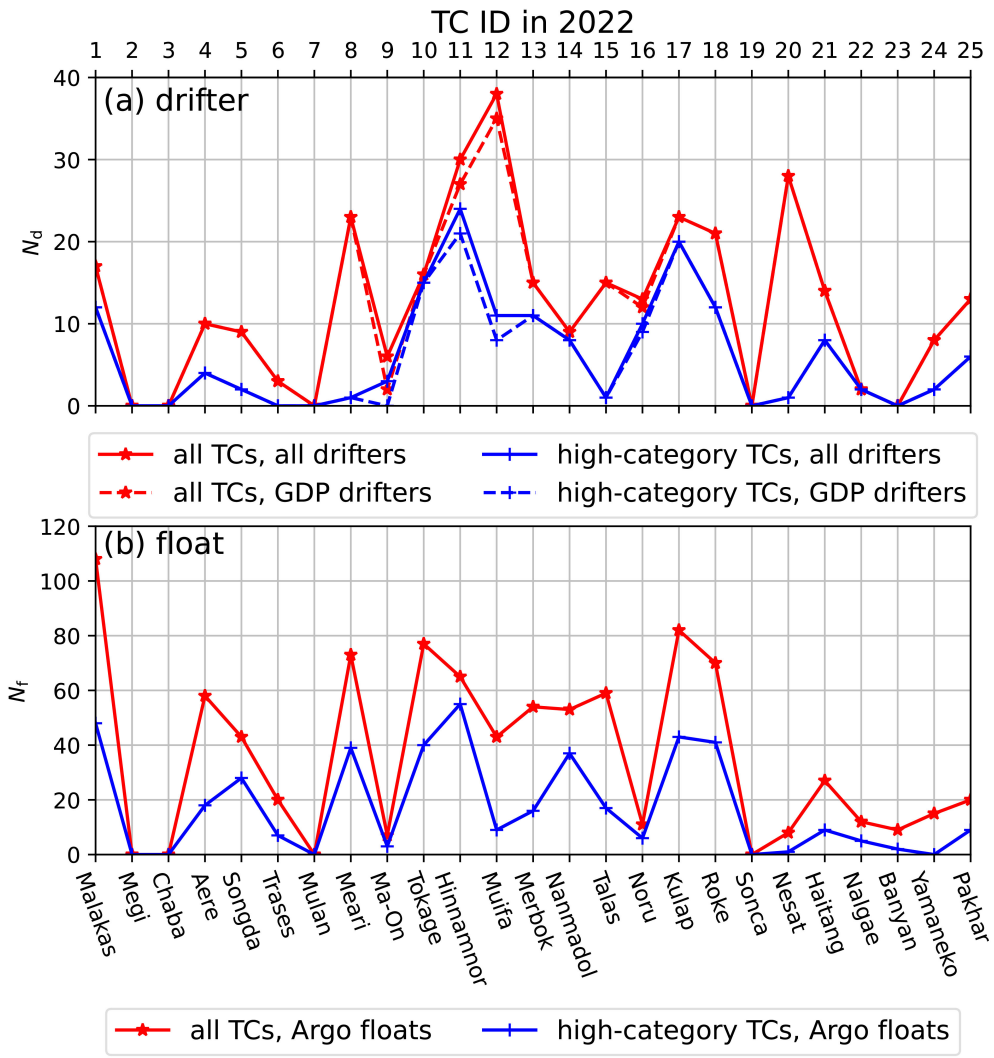

FIGURE 3
The number of **(A)** drifters (N_d) and **(B)** Argo floats (N_f) for each TC in 2022. In **(A)**, solid and dashed lines represent all drifters and only Global Drifter Program's drifters, respectively. The red lines denote all category TCs, while the blue lines represent high-category TCs (maximum sustained wind speeds greater than 17.5 m/s). The bottom abscissa displays the TC names, and the top abscissa indicates the TC IDs in 2022. The search radius is 500 km.

changes in track, warrant special attention and study (Zhang et al., 2023).

The dynamics of surface currents and temperature is also related to the vertical structure of ocean density, a profile typically measured using instruments like Argo floats or similar devices (Sanford et al., 2011; Fu et al., 2014; Oginni et al., 2021). However, the observation status of Argo floats during typhoon events in the western North Pacific remains unclear over the past decade (Wu and Chen, 2012), particularly regarding specific typhoon cases (Chen et al., 2021).

Therefore, the objectives of the present study are threefold: Firstly, to assess the data quality of our surface drifters. Secondly, to investigate the observational capabilities of ocean responses to typhoons in 2022, utilizing both surface drifters and Argo floats. Thirdly, to meticulously examine the ocean observation status during Typhoon Hinnamnor.

TABLE 2 Surface drifters captured by TC Hinnamnor in the western North Pacific during 2022.

Drifter ID	t_0 YYYY-MM-DD HH	x_0 km	V_{max} m/s	ΔSST °C	$\|U_{max}\|$ m/s
67649550	2022-08-29 09	13	41.2	-2.11	0.66
66216740	2022-08-28 15	13	24.4	-0.40	0.31
61286260	2022-08-29 05	22	37.7	-0.86	0.10
68542420	2022-08-28 09	-27	19.3	-0.24	0.08
68542390	2022-08-28 09	-31	19.3	-0.34	0.20
66432050	2022-08-28 15	-61	24.4	—	0.26
68543130	2022-08-29 06	68	38.6	-0.86	0.37
67544100	2022-08-28 18	-72	28.3	-0.15	0.70

(Continued)

TABLE 2 Continued

Drifter ID	t_0 YYYY-MM-DD HH	x_0 km	V_{max} m/s	ΔSST °C	$\|U_{max}\|$ m/s
68543140	2022-08-28 16	99	25.7	-0.05	0.26
68543090	2022-08-28 22	-141	33.4	-0.42	0.14
65701850	2022-08-28 12	-144	20.6	-0.23	0.49
61286230	2022-09-02 12	233	38.6	-0.25	0.31
68542300	2022-08-28 23	-251	34.7	-0.41	0.07
66213760	2022-08-29 11	-287	42.9	—	0.14
66213700	2022-08-30 04	-293	50.6	0.49	0.12
61658680	2022-08-28 17	-325	27.0	-0.39	0.43
30000003	2022-09-02 12	325	38.6	-0.32	0.61
66813190	2022-08-28 00	-331	0.0	0.33	0.63
60616560	2022-08-27 18	345	—	-0.05	0.21
61394350	2022-08-28 03	—	9.0	-0.44	0.11
30000008	2022-09-01 12	-358	51.4	-0.66	0.24
66213720	2022-08-30 03	361	50.2	0.16	0.09
60520110	2022-08-28 02	-370	6.0	0.17	0.28
30000007	2022-09-02 12	399	38.6	-0.94	0.26
66213740	2022-08-29 02	-407	36.0	-0.21	0.27
60753060	2022-08-29 05	-419	37.7	-0.18	0.30
60523120	2022-08-29 15	-433	43.7	0.14	0.13
68542120	2022-08-28 03	438	9.0	0.04	0.34
61297880	2022-08-27 18	-459	—	-0.04	0.19

t_0 is the arrival time of TC. At t_0, x_0 is the cross-track coordinate, V_{max} is the maximum sustain wind speed of TC, ΔSST is the SST change as referred to 1 day before, and $|U_{max}|$ is the current speed. The search radius is 500 km.

2 Materials and method

2.1 Best track of TC

We utilize the best track data provided by the Japan Meteorological Agency (JMA), with a temporal resolution of 6 or 3 hours (case dependent).

TABLE 3 Comparisons between our and Global Drifter Program's (GDP) drifters during TC Hinnamnor.

Variable	Our drifter	GDP's drifter	Δ	*RD*
$\|U\|$ (m/s)	0.31	0.24	0.07	30.23%
θ (°)	-59.89	-43.47	-16.42	—
SST (°C)	29.05	29.95	-0.90	-3.0%

The ID of our drifter is 30000003, and the ID of GDP drifter is 61286230. The transient time is 2022/09/03 12:00:00. The distance between two drifters was 68 km. Δ indicates the difference, *RD* is the relative difference, $|U|$ is the current speed, θ represents the current direction, and SST is the sea surface temperature.

2.2 Surface drifter

We also utilize data from the Global Drifter Program (GDP), with a corresponding temporal resolution of 6 hours. The accuracy of Sea Surface Temperature (SST) in the GDP dataset is reported as 0.05°C, while the accuracy of surface currents is approximately 1 cm/s (Hansen and Poulain, 1996). Meanwhile, we have deployed 8 new surface drifters in the western North Pacific. The data collection period spans from July 19, 2022, to September 24, 2022. These surface drifters record both position and SST, and the data are transmitted to land via the BeiDou satellite system with a 1-hour resolution. The accuracy of our SST and surface current measurements is nearly consistent with that of the GDP.

2.3 Argo float

We also incorporate data from Argo floats, which observe ocean temperature and salinity profiles. These measurements enable us to compute ocean density based on water temperature and salinity. Argo floats typically repeat their profiling every 10 days, although for certain specialized floats, the temporal resolution can approach nearly 1 day (Wada et al., 2014).

3 Results

3.1 Best track

Figure 1 illustrates all TC tracks in 2022, totaling 25 TCs. Table 1 provides details such as start time, lifetime, and intensity (minimum central pressure) of each TC. TC Malakas, occurring in the spring season, exhibited a significant lifetime of 11.75 days with a minimum pressure reaching as low as 945 hPa. Conversely, Megi, also a spring TC, had a much shorter lifespan of 3.25 days. There were 19 TCs during the typical typhoon season (July–October). In a noteworthy case, Hinnamnor originated in the subtropical ocean at (150°E, 20°N). Initially, it moved northwestward, then changed direction to westward and southwestward around 125°E. Subsequently, Hinnamnor made a significant turnaround (125°E, 20°N), followed by a northward and northeastward trajectory. Among other TCs during the typhoon season, Ma-On formed near (130°E, 18°N), moved southwestward, then turned northwestward. It passed over the Philippines Island and entered the South China Sea, eventually making landfall on the China mainland near 110°E. Noru also developed around (130°E, 18°N), moved predominantly westward, crossed the Philippines Island, entered the South China Sea, and ultimately made landfall near (110°E, 18°N). Nesat followed a similar track to Noru, with its eye passing over Luzon Strait. Tracks of Tokage, Merbok, Kulap, Roke, and Haitang predominantly moved northward and northeastward, maintaining distance from land. Post-typhoon season, there were two TCs: Yamaneko in November and Pakhar in December. Both had lifetimes shorter than 3.5 days, with minimum pressures higher than 997 hPa.

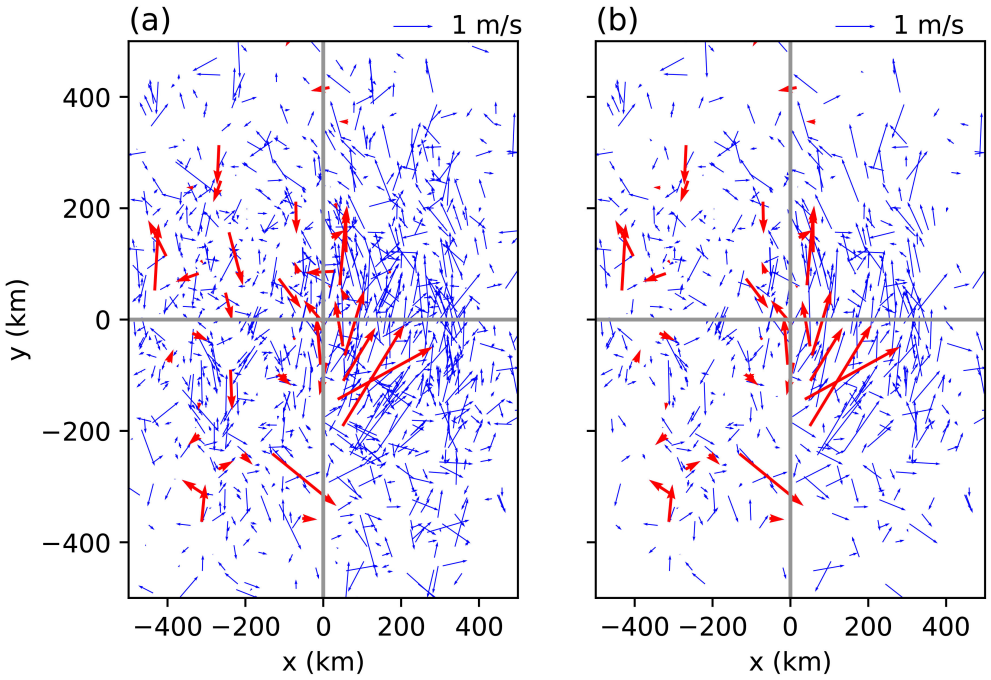

FIGURE 4
Observations of surface currents under TCs in 2022. **(A)** All category TCs, **(B)** high category TCs (maximum sustained wind speeds greater than 17.5 m/s). TC-following coordinate is used, where the *x* coordinate denotes cross-track, and the *y* coordinate signifies along-track. The TC heading direction aligns with the positive *y* direction. Blue arrows represent the Global Drifter Program's surface drifters, while red arrows indicate our surface drifters.

3.2 Surface drifter observation

Figure 2 displays the trajectories of surface drifters during each TC. Figure 3 also depicts the number of drifters within a 500 km search radius. For certain TCs such as Megi, Chaba, Mulan, Sonca and Banyan, no surface drifters were present (Figure 3A). In the case of Meari, although the number of surface drifters exceeded 20, there were only 1 drifter during high category TCs (maximum sustain wind speed exceeds 17.5 m/s). In contrast, the situations during Hinnamnor and Kulap were more promising, with roughly 25 drifters within a 500 km search radius. The drifter count did not sharply decrease with high category TCs. As a result, there were mean 6.1 drifters for high-category TC. During the genesis of Meari, surface drifters provided valuable observations. Initially, there were nearly 20 drifters around the genesis area. However, due to the weak intensity at the beginning, the drifters were not significantly affected by higher category TCs (Figure 3A).

Our drifters significantly contributed to ocean observations. In terms of the number of surface drifters, our deployment increased the count captured by TCs (Figure 3A). Across all intensity levels of TCs, our drifters contributed during Ma-On (2209), Hinnamnor (2211), and Muifa (2212). Specifically, 3 of our drifters were deployed during Hinnamnor (2211). Even during high-category TCs, our drifters continued to function effectively, maintaining a count of 3 during the Hinnamnor event. While our drifters exactly observed the ocean response to Hinnamnor on its track turning point (Figure 2), and they were primarily located on its western side. Table 2 listed the drifter observations during Hinnamnor. The maximum SST cooling in these drifters attained -2.11°C (drifter 67649550), and the maximum surface current was 0.70 m/s (drifter 67544100).

A GDP drifter was in close proximity to ours, allowing for a comparison of transient surface current and temperature measurements, as detailed in Table 3. The minimum distance between the two drifters was 68 km. Our drifter recorded slightly stronger current speeds compared to the GDP drifter, with a relative difference of 30%. The difference in current direction was -16.42°. Furthermore, our drifter recorded a colder SST than the GDP drifter by 0.9°C, suggesting weak disparity in measurements between the two drifters.

Figure 4 further investigates the local coordinates with respect to the TC eye. The *x* coordinate denotes the cross-track direction, while the *y* coordinate represents the along-track direction. Similar to previous studies (Chang et al., 2013), surface current patterns typically exhibit a rightward bias (Chen et al., 2021). The vortex-like pattern and right-side bias are more pronounced in relatively high-category TCs, where the vortex wind forcing is stronger. The surface currents measured by our drifter are also broadly consistent with vortex distribution and right-side bias. It's worth noting the presence of abnormal upward (positive) currents on the left side of the track, likely attributable to background currents, sudden changes in TC trajectory, or localized wind forcing.

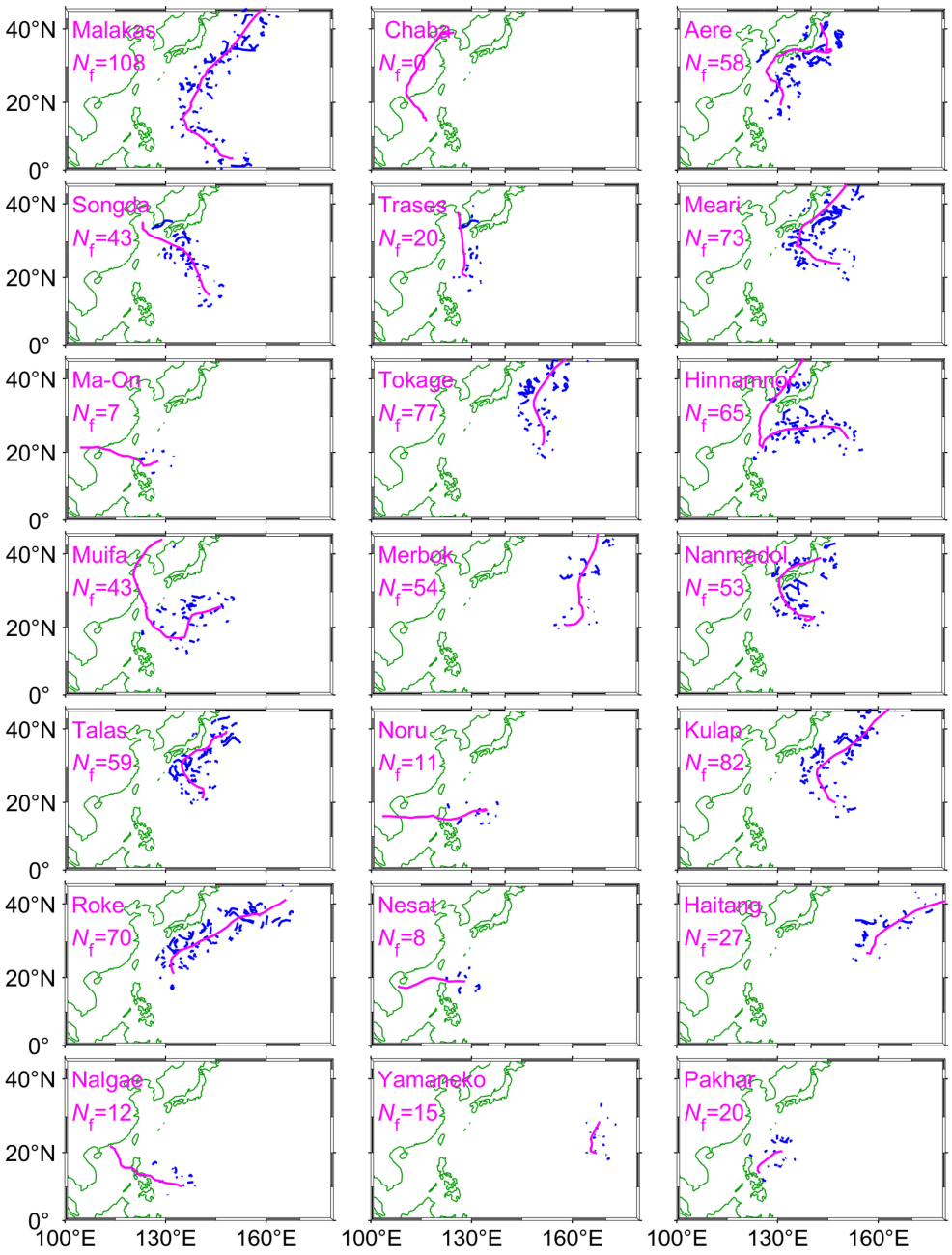

FIGURE 5
An overview of Argo floats during TCs in 2022. The magenta solid line depicts the best track of the TC, while blue solid line represents the trajectory of Argo float. N_f is the number of captured floats. The search radius is 500 km.

3.3 Argo float observation

Argo floats offer a platform for oceanic profiling observations. On average, there were 17.3 Argo floats for high category TC. In the case of specific typhoons, such as Hinnamnor, the number of Argo floats deployed is considerably high (Figure 3). Within a 500 km search radius, nearly 65 Argo floats are captured. After excluding instances of weak TC conditions, approximately 55 Argo floats were found near the TC track (Figure 3). Examining the records of Argo floats during Hinnamnor, it is observed that the floats are primarily located around 25°N (Figure 5).

Figure 6 further illustrates the observational profiles of temperature and salinity during typhoon Hinnamnor. The drifter ID for this data is 2903674, with a minimum distance to the typhoon eye of 78 km. The temporal resolution of this float data is approximately 5 days. A noticeable cooling of SST is observed. Prior to the TC's arrival, the SST was around 30.5°C. During the TC's forcing, the SST decreased to 30.2°C, and post-TC passage, it further dropped to 29.1°C. Therefore, the SST cooling attained -1.4°C after the TC passage. In the vertical profile, the subsurface isothermocline rises towards the sea surface, indicating significant thermocline entrainment. Accordingly, a relatively fresher sea

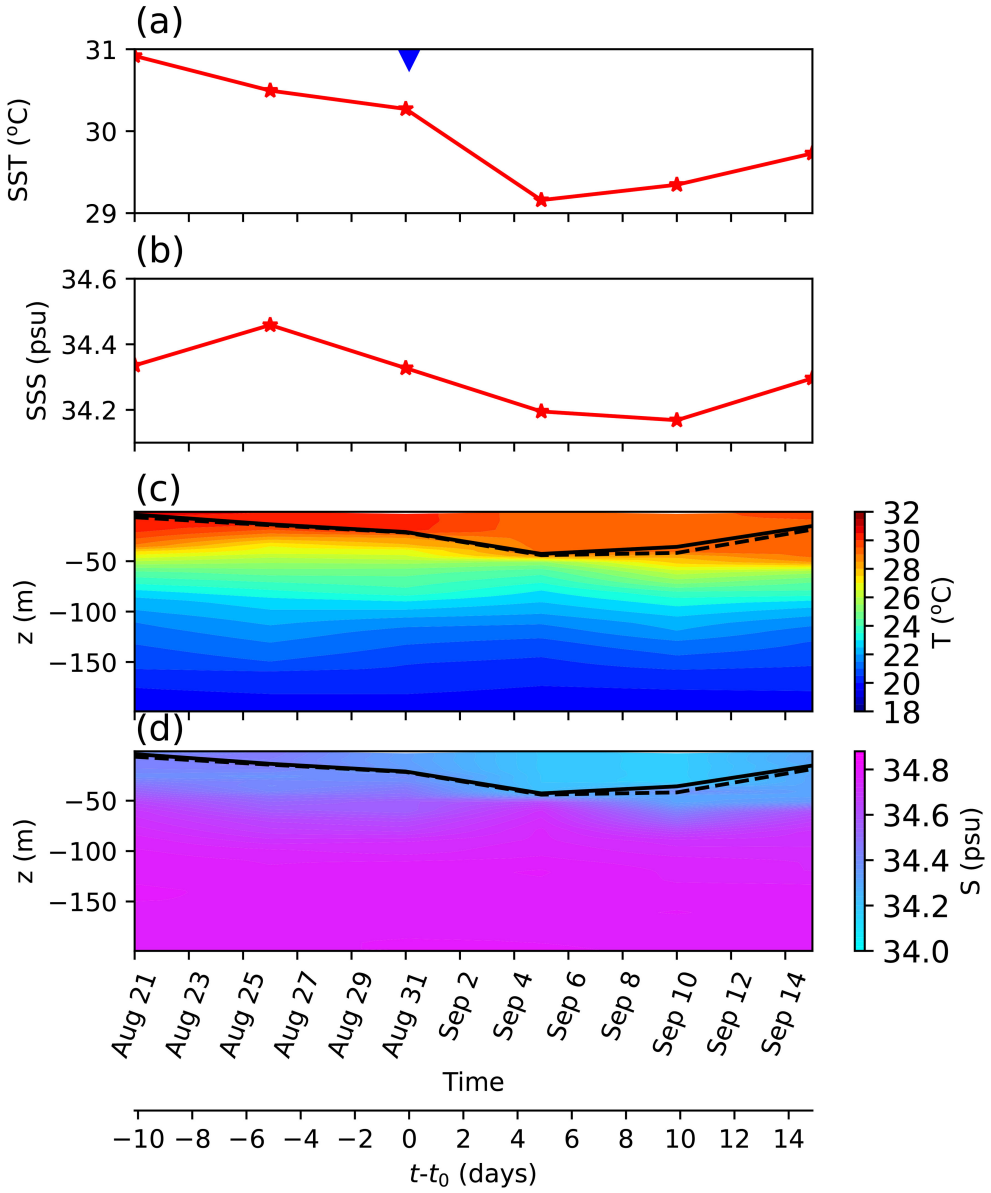

FIGURE 6
Profiles of Argo float during TC Hinnamnor. **(A)** Sea surface temperature (SST), **(B)** sea surface salinity (SSS), **(C)** temperature profiles and **(D)** salinity profiles. Float ID: 2903647. The minimum distance between float and TC is 78 km. In **(A)**, blue triangular marker represents the arrival time of TC. In **(C, D)**, black solid and dashed lines represent mixed-layer depth (MLD) and the isothermal depth (ITD) respectively. t is time, and t_0 is the TC's arrival time.

surface salinity is observed, likely due to surface precipitation. The mixed layer depth (MLD) deepened significantly. At the time of TC forcing, the MLD was approximately 21 m, extending further to 43 m on 5 days after the TC's passage. The isothermal depth (ITD) generally mirrors the behavior of the MLD. The definitions of MLD and ITD used here follow those provided by Wada et al. (2014); Oginni et al. (2021). Table 4 further listed the Argo floats during TC Hinnamnor. At the forcing stage of Hinnamnor, the maximum SST cooling attained -0.53°C (Float 2903642). Meanwhile, the corresponding MLD change was 8.9 m.

For all TCs in 2022, the average number of Argo floats deployed was 36.5. However, for high-category TCs, this number dropped to 17.3. During TCs Malakas, Hinnamnor and Kulap, the number of Argo floats deployed under high-category TC conditions exceeded 40 (Figure 3B). Malakas was observed by greatest number of floats as the number of 108. During TC Aere, a significant number of Argo floats were captured within a 500 km search radius (number is 58). However, the number of Argo floats observed under high-category TCs remained limited, with only 18 floats remaining. TCs Meari and Tokage also captured a considerable number of floats, with a total of 73 and 77 floats, respectively. Notably, for high-category TCs, the number of floats during Meari and Tokage remained nearly 40. Considering Muifa, Nanmadol and Talas, there were some Argo floats around the genesis area. Similarly, 70 Argo floats were captured by Roke, and the Argo floats located at both left and right sides of TC tracks.

10.3389/fmars.2024.1445071

TABLE 4 Argo floats captured by TC Hinnamnor in the western North Pacific during 2022.

Float ID	t_0 YYYY-MM-DD HH	x_0 km	V_{max} m/s	ΔSST °C	ΔMLD m
2903648	2022-08-30 00	3	48.9	-0.05	2.9
2901808	2022-09-05 20	-8	36.0	0.04	0.6
4903637	2022-09-05 23	-25	34.3	-0.17	1.9
4903636	2022-09-05 23	8	34.3	-0.14	0.9
2903705	2022-08-30 05	30	51.0	-0.24	5.0
5906513	2022-08-29 22	-29	48.0	-0.08	-1.1
2903676	2022-08-28 19	-74	29.6	-0.02	-0.8
2903706	2022-08-30 08	77	52.3	-0.05	5.5
2903647	2022-08-31 03	-78	51.4	-0.07	1.9
2903625	2022-08-30 23	-80	52.3	-0.22	7.4
2901811	2022-09-05 18	-81	36.0	0.14	—
2903710	2022-08-29 20	89	47.2	—	—
2903686	2022-08-31 10	-93	51.4	—	—
2903642	2022-09-01 18	73	46.3	-0.53	8.9
2903346	2022-08-30 02	-108	49.7	—	—
2903618	2022-08-28 16	111	25.7	-0.11	1.8
5905847	2022-08-29 06	116	38.6	-0.08	1.4
2901806	2022-09-06 01	-119	33.4	-0.12	-0.0
2903688	2022-08-30 01	-126	49.3	-0.09	0.5
2903649	2022-08-30 05	-129	51.0	-0.01	-0.5
2903709	2022-08-30 14	-145	54.0	-0.30	5.3
2901795	2022-09-06 04	-153	32.6	-0.10	-0.1
2901785	2022-09-06 09	164	15.4	-0.35	-1.0
5906762	2022-08-27 18	—	0.0	-0.04	0.2
2903622	2022-08-28 10	174	19.7	-0.11	1.0
2903707	2022-08-30 06	175	51.4	0.00	1.5
2903645	2022-08-29 11	177	42.9	-0.01	2.8
5904935	2022-08-28 20	-181	30.9	-0.09	0.9
2901791	2022-09-06 08	-195	20.6	-0.25	-0.8
5901937	2022-09-01 18	-137	46.3	-0.15	0.0
2901801	2022-09-06 07	-201	25.7	-0.08	0.0
2903652	2022-08-30 15	203	54.0	-0.05	-1.6
2901810	2022-09-06 06	197	30.9	0.01	1.3
5905061	2022-08-30 00	-203	48.9	-0.15	0.9
2903650	2022-08-27 18	—	0.0	-0.04	0.5
2903687	2022-08-31 07	-217	51.4	-0.11	3.3
2903690	2022-08-30 19	-227	54.0	-0.14	4.1
5906522	2022-08-28 21	232	32.2	-0.06	0.6
2903651	2022-08-27 20	240	0.0	0.02	-0.2
2903695	2022-08-30 22	242	53.2	-0.01	-0.3
2903425	2022-08-28 06	251	18.0	-0.04	0.6
2903626	2022-08-30 05	-287	51.0	-0.04	-0.1

t_0 is the arrival time of TC. At t_0, x_0 is the cross-track coordinate, V_{max} is the maximum sustain wind speed of TC, ΔSST is the SST change as referred to 1 day before, and ΔMLD is the corresponding MLD change. Only x_0 ≤300 km is shown here.

3.4 Integrated observation by surface drifter and Argo float

We examined the transient observations of Typhoon Hinnamnor by combining data from both surface drifters and Argo floats (Figure 7). On the initial day of the typhoon's presence (Day 00), there were 11 surface drifters and 4 Argo floats deployed. By the following day (Day 01), the number of surface drifters had increased to 16, while the number of Argo float decreased to 1. On the subsequent day (Day 02), the count reduced to 7 surface drifters and 1 Argo float. Day 03 saw 2 Argo floats operational, with 1 surface drifter detected. Similarly, on Day 04, 3 Argo floats remained active. Moving to Day 05, 5 surface drifters were operational, with 3 of them belonging to our deployment. Additionally, 1 Argo float was operational. Notably, on this day, the typhoon moved slowly. Day 06 recorded 4 surface drifters, with 3 of them belonging to our deployment, along with 2 Argo floats. On Day 07, only 1 surface drifter was active, and by Day 08, neither surface drifters nor Argo floats were available.

4 Discussion

We deployed 8 surface drifters in the western North Pacific, and some of them were influenced by TCs in 2022. Our surface drifter data are reliable for the following two reasons: Firstly, the spatial pattern under TC-following coordinates emphasizes the vortex distribution, with the current on the right side significantly higher than that on the left side. Secondly, the transient differences between our drifters and GDP drifters are not markedly different. The relative difference in current speed was 30.23%, and the difference in current direction was -16.42°. It is also worth noting that the distance between these two drifters was 68 km (see Table 3).

On average, there were approximately 6.1 drifters deployed during periods of relatively high-category tropical cyclones (with maximum sustained wind speeds exceeding 17.5 m/s), aimed at measuring surface currents and SST (see Figure 3). Additionally, during these high-category TC events, there were an average of 17.3 Argo floats deployed for profiling observations. Given that the typical repeat time of Argo floats is nearly 10 days, the transient

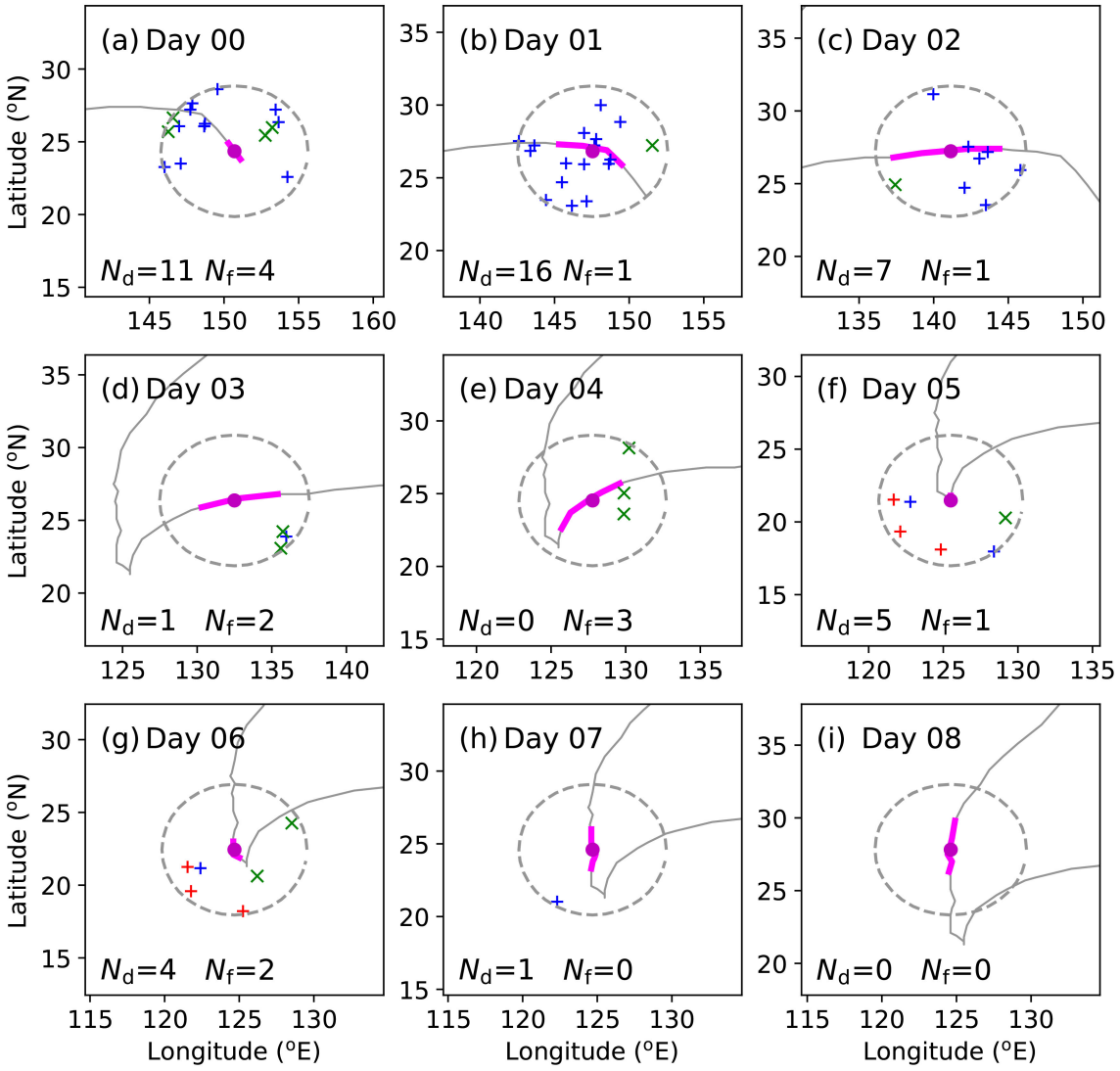

FIGURE 7
Transient integrated observations of ocean response to TC Hinnamnor. TC-following longitude-latitude coordinate is used. Gray solid line is the best track of TC. Magenta line is the TC track in the every day. Magenta circle (marker) represents the TC eye. Gray circle (dashed line) represents 500 km search radius. Blue plus (marker) indicates the surface drifter from Global Drifter Program. Red plus (marker) shows our surface drifter. Green cross (marker) represents the Argo float. N_d and N_f are the numbers of captured surface drifters and floats, respectively.

observations of ocean responses to tropical cyclones are still somewhat limited in the case of TCs.

After integrating the GDP and current surface drifters, the total surface measurement count reached as high as 16 at the beginning of Typhoon Hinnamnor. Our drifters offered new observations of the ocean response to typhoon Hinnamnor, which is particularly notable for its unusual track. Our drifter's locations were within 500 km distance to the turning point of Hinnamnor's track, providing new data on the ocean response to this abruptly turning TC.

Overall, there remains an inadequate observation of tropical cyclone-ocean interactions in the western North Pacific. More surface drifters and Argo floats are required in future endeavors. Meanwhile, the emergence of new unmanned observation platforms presents an opportunity for advancement. Further development should encompass a holistic approach, integrating gliders, unmanned ships/boats, and drifting meteorological buoys as well as present surface drifters and Argo floats (or other Argo-like floats). While there are fewer mooring buoys in the western North Pacific, some are available and should be considered for incorporation in future observational strategies. It is imperative to expand observation methods to provide a more comprehensive understanding of the ocean's response and feedback to TCs.

Data availability statement

The raw data supporting the conclusions of this article will be made available by the authors, without undue reservation.

Author contributions

HH: Conceptualization, Formal analysis, Investigation, Visualization, Writing – original draft. ZL: Investigation, Writing – original draft. SW: Investigation, Writing – original draft. XL: Conceptualization, Writing – review & editing. ZZ: Conceptualization, Writing – review & editing. RT: Writing – review & editing. YW: Writing – review & editing. JS: Writing – review & editing.

Funding

The author(s) declare financial support was received for the research, authorship, and/or publication of this article. This research was supported by the National Natural Science Foundation of China (Grant no. 42227901), the Oceanic Interdisciplinary Program of Shanghai Jiao Tong University (Grant no. SL2020MS030), and the Scientific Research Fund of the Second Institute of Oceanography, MNR (Grand no. JG2301).

Conflict of interest

The authors declare that the research was conducted in the absence of any commercial or financial relationships that could be construed as a potential conflict of interest.

Publisher's note

References

Bender, M. A., Ginis, I., Tuleya, R., Thomas, B., and Marchok, T. (2007). The operational GFDL coupled hurricane–ocean prediction system and a summary of its performance. *Monthly Weather Rev.* 135, 3965–3989. doi: 10.1175/2007MWR2032.1

Cao, Y., Wang, X., and Shao, C. (2022). Global estimate of tropical cyclone-induced diapycnal mixing and its links to climate variability. *J. Geophysical Research: Oceans* 127, e2021JC017950. doi: 10.1029/2021JC017950

Chang, Y.-C., Chen, G.-Y., Tseng, R.-S., Centurioni, L. R., and Chu, P. C. (2013). Observed near-surface flows under all tropical cyclone intensity levels using drifters in the northwestern Pacific. *J. Geophysical Research: Oceans* 118, 2367–2377. doi: 10.1002/jgrc.20187

Chen, H., Li, S., He, H., Song, J., Ling, Z., Cao, A., et al. (2021). Observational study of super typhoon Meranti, (2016) using satellite, surface drifter, Argo float and reanalysis data. *Acta Oceanologica Sin.* 40, 70–84. doi: 10.1007/s13131-021-1702-9

Choi, J. M., and Kim, W. (2018). "Applications of surface velocity current derived from Geostationary Ocean Color Imager (GOCI)," in *2018 OCEANS - MTS/IEEE Kobe Techno-Oceans (OTO)*, IEEE 1–4. doi: 10.1109/OCEANSKOBE.2018.8559174

Deng, X. (2016). *Satellite Altimetry* (Cham: Springer International Publishing), 1–5. doi: 10.1007/978-3-319-02370-058-1

Fan, S., Zhang, B., Perrie, W., Mouche, A., Liu, G., Li, H., et al. (2022). Observed ocean surface winds and mixed layer currents under tropical cyclones: Asymmetric characteristics. *J. Geophysical Research: Oceans* 127, e2021JC017991. doi: 10.1029/2021JC017991

Fu, H., Wang, X., Chu, P. C., Zhang, X., Han, G., and Li, W. (2014). Tropical cyclone footprint in the ocean mixed layer observed by Argo in the northwest Pacific. *J. Geophysical Research: Oceans* 119, 8078–8092. doi: 10.1002/2014JC010316

Gray, W. (1998). The formation of tropical cyclones. *Meteorl. Atmos. Phys.* 67, 37–69. doi: 10.1007/BF01277501

Hansen, D. V., and Poulain, P.-M. (1996). Quality control and interpolations of WOCE-TOGA drifter data. *J. Atmospheric Oceanic Technol.* 13, 900–909. doi: 10.1175/1520-0426(1996)013⟨0900:QCAIOW⟩2.0.CO;2

He, H., Cao, A., Wang, Y., and Song, J. (2022). Evolution of oceanic near-inertial waves induced by typhoon Sarika, (2016) in the South China Sea. *Dynamics Atmospheres Oceans* 100, 101332. doi: 10.1016/j.dynatmoce.2022.101332

He, H., Tian, R., Lyu, X., Ling, Z., Sun, J., and Cao, A. (2024). Annual review of in *situ* observations of tropical cyclone–ocean interaction in the western North Pacific during 2023. *Remote Sens.* 16, 1990. doi: 10.3390/rs16111990

Laurindo, L. C., Mariano, A. J., and Lumpkin, R. (2017). An improved near-surface velocity climatology for the global ocean from drifter observations. *Deep Sea Res. Part I: Oceanographic Res. Papers* 124, 73–92. doi: 10.1016/j.dsr.2017.04.009

Lenain, L., and Melville, W. K. (2014). Autonomous surface vehicle measurements of the ocean's response to tropical cyclone Freda. *J. Atmospheric Oceanic Technol.* 31, 2169–2190. doi: 10.1175/JTECH-D-14-00012.1

Li, Y., Tang, Y., Wang, S., and Li, X. (2023). Rapid growth of tropical cyclone outer size over the western North Pacific. *Remote Sens.* 15, 486. doi: 10.3390/rs15020486

Lumpkin, R., and Johnson, G. C. (2013). Global ocean surface velocities from drifters: Mean, variance, El Niño–Southern Oscillation response, and seasonal cycle. *J. Geophysical Research: Oceans* 118, 2992–3006. doi: 10.1002/jgrc.20210

Oey, L. (2023). A simple model of sea-surface cooling under a tropical cyclone. *J. Mar. Sci. Eng.* 11, 397. doi: 10.3390/jmse11020397

Oginni, T. E., Li, S., He, H., Yang, H., and Ling, Z. (2021). Ocean response to super-typhoon Haiyan. *Water* 13, 2841. doi: 10.3390/w13202841

Prasad, T. G., and Hogan, P. J. (2007). Upper-ocean response to hurricane Ivan in a 1/25° nested Gulf of Mexico HYCOM. *J. Geophysical Research: Oceans* 112, C04013. doi: 10.1029/2006JC003695

Price, J. F. (1981). Upper ocean response to a hurricane. *J. Phys. Oceanography* 11, 153–175. doi: 10.1175/1520-0485(1981)011⟨0153:UORTAH⟩2.0.CO;2

Röhrs, J., Sperrevik, A. K., Christensen, K. H., Broström, G., and Breivik, Ø. (2015). Comparison of HF radar measurements with Eulerian and Lagrangian surface currents. *Ocean Dynamics* 65, 679–690. doi: 10.1007/s10236-015-0828-8

Sanford, T. B., Price, J. F., and Girton, J. B. (2011). Upper-ocean response to hurricane Frances, (2004) observed by profiling EM-APEX floats. *J. Phys. Oceanography* 41, 1041–1056. doi: 10.1175/2010JPO4313.1

Tavakoli, S., Khojasteh, D., Haghani, M., and Hirdaris, S. (2023). A review on the progress and research directions of ocean engineering. *Ocean Eng.* 272, 113617. doi: 10.1016/j.oceaneng.2023.113617

Wada, A., Uehara, T., and Ishizaki, S. (2014). Typhoon-induced sea surface cooling during the 2011 and 2012 typhoon seasons: observational evidence and numerical investigations of the sea surface cooling effect using typhoon simulations. *Prog. Earth Planetary Sci.* 1, 11. doi: 10.1186/2197-4284-1-11

Wang, H., Li, J., Song, J., Leng, H., Wang, H., Zhang, Z., et al. (2023a). The abnormal track of super typhoon Hinnamnor (2022) and its interaction with the upper ocean. *Deep Sea Res. Part I: Oceanographic Res. Papers* 201, 104160. doi: 10.1016/j.dsr.2023.104160

Wang, Q., Zhao, D. J., Duan, Y. H., Guan, S. D., Dong, L., Xu, H. X., et al. (2023b). Super typhoon Hinnamnor (2022) with a record-breaking lifespan over the western North Pacific. *Adv. Atmos. Sci.* 40, 1558–1566. doi: 10.1007/s00376-023-2336-y

Wu, Q., and Chen, D. (2012). Typhoon-induced variability of the oceanic surface mixed layer observed by Argo floats in the western North Pacific Ocean. *Atmosphere-Ocean* 50, 4–14. doi: 10.1080/07055900.2012.712913

Yu, C., Yang, Y., Yin, X., Sun, M., and Shi, Y. (2020). Impact of enhanced wave-induced mixing on the ocean upper mixed layer during typhoon Nepartak in a regional model of the Northwest Pacific Ocean. *Remote Sens.* 12, 2808. doi: 10.3390/rs12172808

Zhang, H., Liu, Y., Liu, P., Guan, S., Wang, Q., Zhao, W., et al. (2023). Enhanced upper ocean response within a warm eddy to typhoon Nakri (2019) during the sudden-turning stage. *Deep Sea Res. Part I: Oceanographic Res. Papers* 199, 104112. doi: 10.1016/j.dsr.2023.104112